PHYSICAL REVIEW B **82**, 100101(R) (2010)

# Nucleation mechanism of the $\sigma$-to-$\alpha$ phase transition in $Fe_{1-x}Cr_x$

Alice Mikikits-Leitner,* Bogdan Sepiol, and Michael Leitner
*Fakultät für Physik, Universität Wien, Strudlhofgasse 4, 1090 Wien, Austria*

Jakub Cieslak and Stanisław M. Dubiel
*Faculty of Physics and Computer Science, AGH University of Science and Technology, PL-30-059 Kraków, Poland*
(Received 5 July 2010; published 15 September 2010)

This Rapid Communication reports on Mössbauer-spectroscopy measurements of the kinetics of the $\sigma$-to-$\alpha$ phase transition in the system Fe-Cr. By isothermally annealing samples of the compositions $Fe_{53.8}Cr_{46.2}$ and $Fe_{51}Cr_{49}$ at temperatures between 820 and 855 °C the authors gained information about the kinetics of the phase transition in terms of the Johnson-Mehl-Avrami-Kolmogorov equation. The obtained values for the Avrami exponent allow to draw conclusions about the type of nucleation mechanism. The behavior of the Avrami exponent for near-critical temperatures and for higher temperatures indicates a change in the nucleation mechanism with $T$-$T_c$.

DOI: 10.1103/PhysRevB.82.100101 PACS number(s): 64.60.Q−, 64.70.kd

We investigated the kinetics of the $\sigma$-to-$\alpha$ phase transition in the system iron-chromium (Fe-Cr). As Fe-Cr is the base alloy of stainless steels, it is of particular importance for several branches of industry (e.g., development of prospective fusion reactors and oil refinery plants). The wide application of stainless steels is, in particular, due to their resistance to corrosion, even at high temperatures and to radiation damage. However, the $\sigma$ phase, which may appear in stainless steels as well as in the binary Fe-Cr system, already at small volume fractions highly deteriorates the properties of the materials. This is not only due to the $\sigma$ phase's own high brittleness but also to its tendency to deplete the surrounding matrix of Cr and therefore to lower the corrosion and radiation resistance of the whole component. Because of these reasons the thermodynamics and kinetics of the $\sigma/\alpha$ phase boundary are of high relevance to industry. Here we treat the special case of the binary system Fe-Cr as a well-defined model system.

The $\sigma$ phase in the system Fe-Cr is stable at temperatures less than $T_c \sim 820$ °C and at iron contents between 50–57 at. % (Ref. 1) (see Fig. 1). The crystallographic structure of the $\sigma$ phase was established by Bergman and Shoemaker[3] as tetragonal, belonging to the space-group-type $D_{4h}^{14}$—$P4_2/mnm$. The unit cell consists of 30 atoms, these are distributed over five inequivalent sites. A tendency of the Fe atoms to occupy specific sublattices is discernible.[4,5]

The formation of the $\sigma$ phase from the $\alpha$ matrix phase in stainless steels[6,7] as well as the retardation of the formation of the $\sigma$ phase in Fe-Cr by doping with appropriate amounts of aluminum or titanium was extensively investigated.[8,9] In this Rapid Communication, we investigate the reverse transition in the system Fe-Cr, i.e., the decay of the $\sigma$ phase. We particularly focus on the transformation mechanism and its temperature dependence. This is in contrast to previous investigations on high-chromium ferritic steels,[6,7] which primarily focused on phenomenological questions, such as the time-temperature dependence of the phase transition.

The samples of $Fe_{53.8}Cr_{46.2}$ and $Fe_{51}Cr_{49}$ were prepared by melting appropriate amounts of iron (99.95% purity) and chromium (99.5% purity) in a vacuum induction furnace. Subsequently, the resulting ingots were cut into cubes of the dimensions $(5\ \text{mm})^3$. These cubes were then homogenized by vacuum annealing for 24 h at 1000 °C and finally water quenched. The exact chemical compositions of the samples were determined by electron probe microanalysis. The concentrations of Fe and Cr were evaluated as an average over five values measured at various spots of the sample. The samples, consisting of the $\alpha$ phase after the quench, were then rolled into sheets of the thickness of about 10 $\mu$m. Afterwards, these foils were cut into pieces of $(5\ \text{mm})^2$, which were finally transformed from the $\alpha$ into the $\sigma$ phase by an isothermal vacuum anneal at 700 °C for 24 h.

We studied the kinetics of the $\sigma$-to-$\alpha$ phase transition as measured by transmission Mössbauer spectroscopy, where we used a standard spectrometer and a $^{57}$Co/Rh source. Mössbauer spectroscopy seems to be the optimal tool to distinguish between the two phases since at room temperature the $\sigma$ phase is paramagnetic whereas the $\alpha$ phase is ferromagnetic, allowing the contributions from the respective phases to be unambiguously determined. Furthermore, Mössbauer spectroscopy generically measures bulk samples without being affected by polycrystallinity. This is in contrast to, e.g., x-ray diffraction.

The samples, which consisted of the $\sigma$ phase after the preparation described above, were alternately isothermally vacuum annealed at a certain temperature (at which the $\alpha$ phase is thermodynamically stable) and *ex situ* measured in

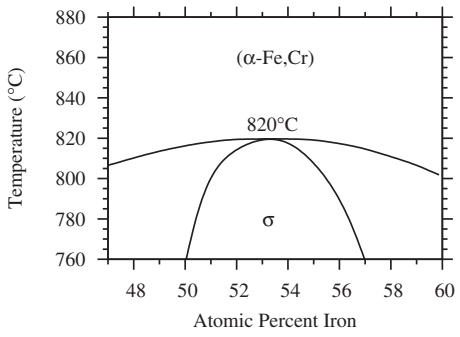


FIG. 1. The relevant part of the phase diagram of Fe-Cr (redrawn from Ref. 2).

 

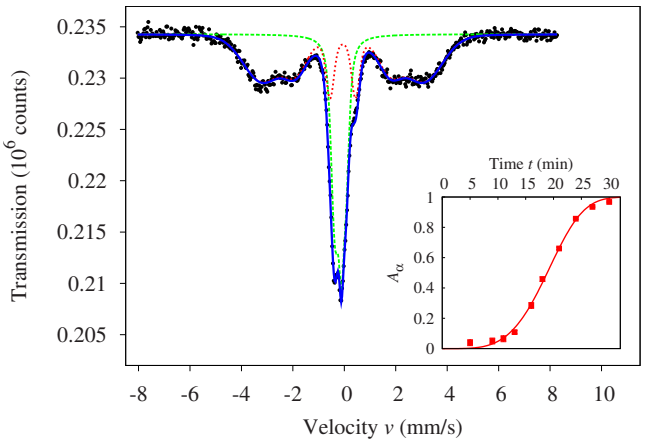


FIG. 2. (Color online) The main panel shows the Mössbauer transmission spectrum of the sample $Fe_{51}Cr_{49}$ annealed at $T=835$ °C for an annealing time $t=21$ min ($A_\alpha=66.1\%$). $A_\alpha$ constitutes the corrected $\alpha$ fraction present in the sample, see Eq. (1). The subspectrum originating from the $\sigma$ phase is green (dashed line) and the one from the $\alpha$ phase is red (dotted line). The fit, which is the sum of these subspectra, is blue (full line). The inset shows the kinetics of the transformation at this composition and temperature. The line stands for the best fit in terms of Eq. (3) with the following values for the fit parameters: $n=4.2\pm0.2$ and $\tau=(20.6\pm0.2)$ min.

transmission by Mössbauer spectroscopy. In this way we obtained sequences of spectra (corresponding to the annealing times) for various temperatures. The correspondence of the temperature felt by the thermocouple with the actual temperature of the sample in the furnace was calibrated via the melting points of tin, aluminum, and silver.

A spectrum obtained from a sample undergoing the $\sigma$-to-$\alpha$ phase transition consists of two subspectra, originating from the two phases. Figure 2 shows a typical example of a transmission spectrum. Since the $\sigma$ phase is paramagnetic, its spectrum consists of a pseudosingle-line pattern (spectral area $S_\sigma$), composed of the contributions from the Fe atoms on the different chemically inequivalent sites. The spectrum of the $\alpha$ phase, however, shows features characteristic for a magnetic phase, namely, a broadened sextet (spectral area $S_\alpha$), where the broadening is due to the random occupations of the neighboring sites of the Fe atoms. Fitting was done by the program RECOIL, which models the hyperfine parameters of the respective sites via Gaussian distributions.[10] For a given Mössbauer spectrum we determined the areas of the subspectra $S_\sigma$ and $S_\alpha$ by fitting the theoretical expressions for the respective models. The amount of the $\alpha$ phase in such a spectrum is then given by

$$A_\alpha = \frac{S_\alpha f_\sigma}{S_\alpha f_\sigma + S_\sigma f_\alpha}, \tag{1}$$

where $f_\alpha$ and $f_\sigma$ denote the Lamb-Mössbauer factors for the $\alpha$ and the $\sigma$ phases, respectively. We made use of the relation between the two Lamb-Mössbauer factors established in Ref. 11: $f_\alpha=0.87f_\sigma$.

The theory of the time dependence of the volume fraction of the growing phase during a phase transition was developed by Kolmogorov,[12] Johnson and Mehl,[13] and Avrami.[14] They supposed the nuclei of the emerging phase to be spherical and the radius of a nucleus to be a convex function of time $t$. Under these assumptions the transformed fraction $A_\alpha$ as a function of time $t$ is given by the Johnson-Mehl-Avrami-Kolmogorov (JMAK) equation

$$A_\alpha(t) = 1 - \exp\left[-\int_0^t I(t')V(t-t')dt'\right], \tag{2}$$

where $I(t')$ denotes the nucleation rate per unit volume and $V(t-t')$ the volume of an $\alpha$ nucleus nucleated at a time $t'$.

A power-law form of $V(t)$, as it is conventionally assumed, allows Eq. (2) to be written in the form

$$A_\alpha(t) = 1 - \exp[-(t/\tau)^n]. \tag{3}$$

The variable $\tau$ denotes the time constant of the transformation, which strongly depends on the temperature $T$.

By $n$ we denote the Avrami exponent, which is determined by the nucleation and growth mechanisms. Hence from the values of $n$, which usually vary between 1 and 4 and can also be noninteger, one can draw conclusions about the type of transformation mechanism at work. Our measurements show that not only the time constant $\tau$ depends on the temperature but also the Avrami exponent $n$ and thus the transformation process. For an overview of the application of the JMAK theory to the interpretation of experimental results see, e.g., Ref. 15 and the references therein.

The kinetics of the samples $Fe_{51}Cr_{49}$ and $Fe_{53.8}Cr_{46.2}$ for different annealing temperatures were evaluated in two steps: first, we fitted the Mössbauer spectra to obtain the amount $A_\alpha(t)$ of the $\alpha$ phase in the sample depending on the annealing time $t$. Subsequently, the $A_\alpha(t)$ values for each temperature were fitted in terms of the JMAK equation. This is illustrated in the inset of Fig. 2, which shows the kinetics of the phase transition in the sample $Fe_{51}Cr_{49}$ at the annealing temperature of $T=835$ °C. By fitting these data in terms of Eq. (3) we got values for the best-fit kinetics parameters: $n=4.2\pm0.2$ and $\tau=(20.6\pm0.2)$ min. Similarly we obtained values for $n$ and $\tau$ corresponding to various annealing temperatures and to the different Fe contents in the sample, see Table I and Figs. 3 and 4.

Figure 3 visualizes the behavior of $\tau$, the time constant of the transformation as a function of the temperature $T$ and for two different Fe contents. The estimated error bars as obtained from the fit of the transformation kinetics are smaller than the symbols. The scatter of the data points, especially at the lower temperatures, has a much larger magnitude: this is a clear indication that the transformation kinetics depend on the actual sample microstructure. This dependence is obviously quite pronounced, as the preparation procedures were the same for each sample. The influence of the Fe content on the temporal scale of the transformation is clearly discernible, though: the $\alpha$ phase emerges faster in the sample with the higher Fe content. This is a surprising finding because the $\sigma$ phase should actually be more stable at this composition (see Fig. 1). We can only speculate on the reasons for this behavior here, a possible explanation would be an enhanced mobility of the $\sigma$-$\alpha$ interface with increasing Fe content.

TABLE I. Values of the parameters $n$ and $\tau$ corresponding to the different Fe contents in the sample and to the various annealing temperatures. The − sign indicates that the kinetics has not been measured at the corresponding temperature.

| | $Fe_{51}Cr_{49}$ | | $Fe_{53.8}Cr_{46.2}$ | |
|---|---|---|---|---|
| $T$ (°C) | $n$ | $\tau$ (min) | $n$ | $\tau$ (min) |
| 820 | 1.3(1) | 304.7(13) | 1.63(5) | 35.7(5) |
| 822 | – | – | 2.1(3) | 36.9(14) |
| 825 | 2.1(3) | 44.3(14) | 3.2(3) | 12.5(2) |
| 830 | 2.3(2) | 19.7(3) | 3.3(2) | 7.5(1) |
| 835 | 4.2(2) | 20.6(2) | 3.2(5) | 4.2(2) |
| 840 | 5.0(3) | 14.7(2) | – | – |
| 845 | 2.3(3) | 7.2(3) | – | – |
| 850 | 3.9(4) | 4.3(1) | – | – |
| 855 | 3.4(5) | 1.8(1) | – | – |

We now turn to the dependence of $\tau$ on the annealing temperature $T$. At first glance it looks tempting to fit the obtained values of $\tau(T)$ by the Arrhenius form, especially at the higher temperatures. This would be incorrect, however, which can be seen by the fact that $\tau(T)$ has to diverge at the critical temperature $T_c$. A correct model would have to take into account the effects of both nucleation and growth. In the classical nucleation theory the energy needed for nucleating a new phase is a function of the interfacial energy between $\sigma$ and $\alpha$ and the difference in free enthalpy between the phases. As the latter goes to zero with $T$-$T_c$, the activation energy diverges. The behavior is further complicated by the fact that the nucleation mechanism itself changes, as discussed below.

We estimate the accuracy of our temperature calibration at 2 °C. We observed at all our measurements a complete transformation of the sample into the $\alpha$ phase, therefore all investigated points lie in the single-phase region of ($\alpha$-Fe,Cr). This would imply that the critical temperature $T_c$ lies below our lowest annealing temperature of 820 °C. Reference 2 claims $T_c$=820 °C, which is consistent with our observations within the estimated errors. However, we can definitely rule out older findings of higher critical temperatures, cp. Ref. 16 with $T_c$=830 °C.

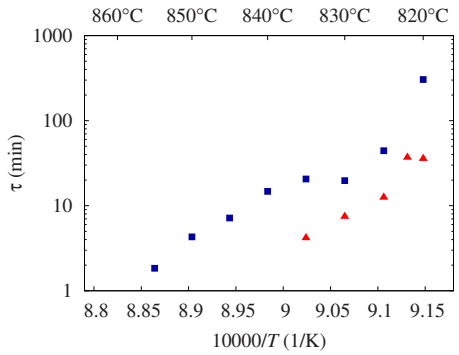


FIG. 3. (Color online) The time constant $\tau$ of the transformation for the samples $Fe_{51}Cr_{49}$ (■, blue) and $Fe_{53.8}Cr_{46.2}$ (▲, red).

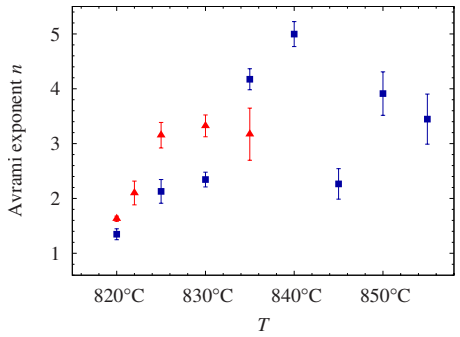


FIG. 4. (Color online) Avrami exponent $n$ of the samples $Fe_{51}Cr_{49}$ (■, blue) and $Fe_{53.8}Cr_{46.2}$ (▲, red) for different annealing temperatures.

The most interesting finding of our investigations is presented in Fig. 4. The Avrami exponent $n$ shows a systematic variation with temperature. For high temperatures, the values of $n$ scatter around a value between 3 and 4. On the other hand, in the temperature range ~820–830 °C, i.e., for temperatures near the critical temperature $T_c$, the Avrami exponent $n$ shows a clear decrease with temperature to values between 1 and 2. For being able to interpret these values we have to develop a microscopic picture of the $\sigma$-to-$\alpha$ transformation.

The $\alpha$ phase has a bcc structure, where there are no preferred sublattices for the Fe and Cr atoms. However, according to Hennion[17] and Mirebeau *et al.*,[18] the occupations of neighboring lattice sites are not independent, a tendency toward building clusters of Fe, respectively, Cr atoms can be observed. In the $\sigma$ phase, on the other hand, as mentioned in the beginning, the Fe atoms prefer to occupy specific lattice sites. The movement of the interface between the $\sigma$ and the $\alpha$ phases has to involve therefore a rearrangement of the Fe and Cr atoms, which will be effected by short-range diffusion. On a coarser scale, the atomic concentrations in the two phases are the same, so no long-range mass transport is necessary. For these reasons we expect the growth of the $\alpha$ nuclei to be interface controlled.

Assuming the above-mentioned growth mechanism we are now able to interpret the values of the Avrami exponent $n$. With a constant velocity of the $\sigma/\alpha$ interface the volume of an $\alpha$ nucleus grows with $V(t) \propto t^d$, where $t$ is the nucleus' age and $d$ denotes the dimension of the growth. Given a constant nucleation rate per unit volume $I(t)$, the special case of an Avrami exponent equal to 4 therefore indicates that the growth of the $\alpha$ nuclei is three-dimensional ($d$=3). Lower values of $n$ correspond to a decreasing nucleation rate and/or a growth of lower dimensionality.[19]

Turning to our results, we can now shed light on the variation in the Avrami exponent $n$ with temperature. The values of $n$ in the temperature region above ~835 °C likely indicate homogeneous nucleation and three-dimensional growth. We interpret the apparent tendency for values a bit below 4 as being due to a decreasing nucleation rate, as in the initial stage of the transformation there will be enhanced nucleation at certain favorable sites (e.g., lattice defects). This picture changes as we come nearer to the critical temperature. We do not claim here that we can pinpoint the exact

dimensionality of the growth for near-critical temperatures but it is obvious that here the nucleation rate decreases with time and/or the dimensionality of the growth is lower. Both options point to heterogeneous nucleation. The favorable nucleation sites have a certain geometry (grain edges or boundaries), leading to a growth of the $\alpha$ grains into the $\sigma$ grains of lower dimensionality (2 or 1, respectively) and to a vanishing nucleation rate at positive times (as the favorable sites will be nucleated at the very beginning). Another argument for a changing over from homogeneous to heterogeneous nucleation is the scatter of the transformation time constants in Fig. 3. The scatter seems to be higher at near-critical temperatures, in line with the fact that the actual sample microstructure will affect the transformation only in the case of heterogeneous nucleation.

From the thermodynamic viewpoint the observed behavior is quite plausible. At temperatures far from the critical temperature the energy necessary to nucleate an $\alpha$ grain in the $\sigma$ matrix is comparatively small and as the grain boundaries/edges make up only a very small fraction $p$ of the sample volume, the nucleations in the matrix will dominate. When the temperature approaches the critical temperature, however, the nucleation energies and concomitantly the preference for nucleation in the boundaries/edges rise, until the ratio of the respective Boltzmann factors eventually becomes larger than $p^{-1}$, leading to heterogeneous nucleation. This dependence of the nucleation mechanism on the ratio of the difference in the free energies of the two phases and $k_BT$ has also been demonstrated via phase-field simulations in Ref. 20.

In conclusion, we reported here a study of the $\sigma$-to-$\alpha$ phase transition in the system Fe-Cr for near-critical temperatures, where we have analyzed the kinetics of the phase transition in terms of the Johnson-Mehl-Avrami-Kolmogorov equation. The main finding is a crossover from homogeneous nucleation of the $\alpha$ phase at higher temperatures to a heterogeneous nucleation, probably at grain boundaries or edges, at near-critical temperatures. We plan to complement the investigations presented here with their counterpart, the near-critical behavior of the $\alpha$-to-$\sigma$ transformation, in order to be able to present a comprehensive picture of the $\sigma/\alpha$ phase equilibrium in the system Fe-Cr.

*alice.mikikits-leitner@univie.ac.at

[1] A. J. Cook and F. W. Jones, J. Iron Steel Inst., London **148**, 217 (1943).
[2] V. P. Itkin, *Phase Diagrams of Binary Iron Alloys* (ASM International, Materials Park, Ohio, 1993), pp. 102–129.
[3] G. Bergman and D. P. Shoemaker, Acta Crystallogr. **7**, 857 (1954).
[4] H. L. Yakel, Acta Crystallogr., Sect. B: Struct. Sci. **39**, 20 (1983).
[5] J. Cieślak, M. Reissner, S. M. Dubiel, J. Wernisch, and W. Steiner, J. Alloys Compd. **460**, 20 (2008).
[6] J. W. Elmer, T. A. Palmer, and E. D. Specht, Metall. Mater. Trans. A **38**, 464 (2007).
[7] R. Magnabosco, Mater. Res. **12**, 321 (2009).
[8] A. Blachowski, J. Cieślak, S. M. Dubiel, and B. Sepiol, Intermetallics **8**, 963 (2000).
[9] A. Blachowski, S. M. Dubiel, J. Zukrowski, J. Cieślak, and B. Sepiol, J. Alloys Compd. **313**, 182 (2000).
[10] D. G. Rancourt and J. Y. Ping, Nucl. Instrum. Methods Phys. Res. B **58**, 85 (1991).
[11] J. Cieślak, S. M. Dubiel, and B. Sepiol, Hyperfine Interact. **126**, 187 (2000).
[12] A. N. Kolmogorov, Bull. Acad. Sci. USSR, Math. Ser. **1**, 355 (1937).
[13] W. A. Johnson and R. F. Mehl, Trans. Am. Inst. Min., Metall. Pet. Eng. **135**, 416 (1939).
[14] M. Avrami, J. Chem. Phys. **7**, 1103 (1939); **8**, 212 (1940); **9**, 177 (1941).
[15] C. W. Price, Acta Metall. Mater. **38**, 727 (1990).
[16] O. Kubaschewski, *Iron-Binary Phase Diagrams* (Springer, Berlin, 1982).
[17] M. Hennion, J. Phys. F: Met. Phys. **13**, 2351 (1983).
[18] I. Mirebeau, M. Hennion, and G. Parette, Phys. Rev. Lett. **53**, 687 (1984).
[19] J. W. Christian, *The Theory of Transformations in Metals and Alloys, Part I*, 3rd ed. (Pergamon Press, Oxford, United Kingdom, 2002), Chap. 12, pp. 529–538.
[20] M. Castro, Phys. Rev. B **67**, 035412 (2003).